EPJ Web of Conferences **5**, 06008 (2010)
DOI:10.1051/epjconf/20100506008

Analysis, optimization and implementation of a variable retardance based polarimeter

A. Peinado[1], A. Lizana[1], J. Vidal[1,2], C. Iemmi[2], A. Márquez[3], I. Moreno[4] and J. Campos[1]

[1]Dept. of Physics, Universitat Autònoma de Barcelona, Bellaterra, Spain
[2] ALBA Synchrotron Light Source Facility, Cerdanyola del Vallès, Spain
[3]Dept. of Physics, Universidad de Buenos Aires, Buenos Aires, Argentina
[4]Dept. of Physics, Ing. Sistemas y Teoría de la Señal, Univ. Alicante, Alicante, Spain
[5]Dept. de Ciencia de Materiales, Optica y Tecnología de la Señal, Univ. Miguel Hernandez, Elche, Spain

Abstract. We present a comprehensive analysis, optimization and implementation of a Stokes polarimeter based on two liquid crystals acting as variable retarders. For the optimization process, the Conditional Number or the Equally Weighted Variance indicators are applied and compared as a function of different number of polarization analyzers. Moreover, some of the optimized polarimeter configurations are experimentally implemented and the influence of small experimental deviations from the optimized configuration values on the amplification of the Stokes component error is also studied. Some experimental results obtained by using the implemented polarimeters, when measuring different incidence states of polarization, are provided.

1 Introduction

Polarimetric information is fundamental in a large number of optical applications as in medical optics [1], astronomy [2], material characterization [3], among others. The basic instrument to perform polarimetric measurements is a polarimeter. One type of polarimeters are the complete Stokes polarimeters [4], which are devices capable to fully determine the polarimetric information of a given light beam.

Liquid crystal materials have proved to be birefringent materials capable to modify their retardance values as a function of the addressed voltage. As a consequence, they are nowadays employed in polarimeter implementations [5-7]. Moreover, in order to minimize the amplification of noise (going from radiometric measurements to the state of polarization detection), an optimization procedure is required.

In this work, we compare the sensitivity to data redundancy of two well-known indicators useful to perform optimizations: the Condition Number (*CN*) [8] and the Equally Weighted Variance (*EWV*) [9]. Afterwards, an optimization procedure based on these indicators is applied, obtaining therefore some optimized Stokes polarimeter configurations as a function of different numbers of polarization analyzers. Because implementations imply obtaining small deviations from theoretical values, a study of the impact of these deviations in the conditioning of the system is also provided. Finally, different Stokes polarimeter configurations are experimentally implemented and tested by measuring light beams with different state of polarizations. The results obtained are compared with those provided by a commercial polarimeter.

The outline of this work is as it follows. In section 2, a mathematical description of Stokes polarimeters and a review of two indicators (the *CN* and the *EWV*) useful to perform polarimeter optimizations are described. In section 3, the sensitivity of *CN* and *EWV* to the number of polarization analyzers is studied. After performing the optimization procedure, some optimized complete polarimeter configurations are obtaining, each one corresponding to a different number of polarization analyzers. Finally, we study the influence of slight deviations from the theoretical polarization analyzers of polarimeters within the conditioning of a system. Stokes polarimeter configurations previously obtained in section 3, are experimentally implemented in section 4. Polarimeters have been tested by measuring different known states of polarization and the results obtained have been compared to those obtained with a commercial polarimeter. Finally, conclusions are presented in section 5.

2 Mathematical polarimeter description and optimization criteria review

There exist different mathematical formalisms useful to describe polarimeters, such as those developed by Jones

[10] or Berreman [11]. The choice of the most suitable mathematical formalism highly depends on the application for which the polarimeter is designed. In this work, we use the Mueller-Stokes (M-S) formalism because it takes into account depolarized light and readily allows determining the state of polarization (SOP) of a light beam just by taking intensity measurements behind a Polarization State Detector (PSD).

In the M-S notation [12] whereas Stokes vectors $\boldsymbol{S}$ (formed by four real parameters) fully describe the state of polarization of light beams, the interaction of light beams with polarizing samples is described by means of Mueller matrices *M*. In fact, Mueller matrices are 4x4 real matrices relating the incident $\boldsymbol{S}_{\text{in}}$ and the exiting $\boldsymbol{S}_{\text{ex}}$ Stokes vectors as it follows:

$$\boldsymbol{S}_{\text{ex}} = \text{M}\boldsymbol{S}_{\text{in}} \tag{1}$$

The first component of the exiting Stokes vector corresponds to the power of the light beam which is transmitted, reflected or scattered by the polarizing sample. If the matrix *M* describes a particular configuration of the PSD, the exiting power can be obtained by simply projecting the incident SOP onto the SOP described by the first row of *M* (i.e. the SOP that gives a maximal power when detected by the specific PSD configuration).

By taking radiometric measures corresponding to the projection of a given incident state of polarization $\boldsymbol{S}$ onto different configurations of the PSD (i.e. different polarization analyzers) the following linear equation system is obtained:

$$\boldsymbol{I} = \text{A}\boldsymbol{S} \tag{2}$$

where $\boldsymbol{I}$ is a nx1 column vector containing the set of radiometric measurements and *A* is a nx4 matrix whose rows are the Stokes parameters of the SOP fully transmitted at the different polarization analyzers.

If the polarization analyzer matrix *A* and the measures vector $\boldsymbol{I}$ are both known, the value of $\boldsymbol{S}$ can be obtained just by solving Eq. (2). Note that because Stokes vectors are formed by four real parameters, for a fully polarimetric description of the solution $\boldsymbol{S}$, a minimum number of four independent polarization analyzers are required.

In addition, we can distinguish two different situations by taking into account if the number *n* of polarization analyzers is equal or higher than four. On the one hand, when the matrix *A* of Eq. (2) is a non-singular square matrix (*n*=4), its inverse A^{-1} exists and it is unique, leading to Eq. (3). On the other hand, if more than four polarization detectors are used (*n*>4), *A* is a *n*x4 rectangular matrix and in general no solution exists. In this last case, it is possible to find the solution by minimizing the mean square error by making use of the pseudoinverse $\widetilde{A}^{-1}$, which is defined in Eq. (4):

$$\boldsymbol{S} = \text{A}^{-1}\boldsymbol{I} \tag{3}$$

$$\boldsymbol{S} = \left(\text{A}^{\text{T}}\text{A}\right)^{-1}\text{A}^{\text{T}}\boldsymbol{I} = \widetilde{\text{A}}^{-1}\boldsymbol{I} \tag{4}$$

where A^{-1}, A^{T} and $\widetilde{A}^{-1}$ are respectively the inverse, the transpose and the pseudoinverse of the matrix *A*.

Therefore, according to the matrix *A*, we can use Eq. (3) or Eq. (4) to obtain an experimental measurement of the incident SOP.

There exist an infinite number of matrices *A* enclosing a minimum of four independent polarization analyzers, and so, being able to describe complete polarimeters. However, in presence of noise in the radiometric measurements, the error amplification on the solution $\boldsymbol{S}$ strongly depends on the specific chosen matrix *A*. When implemented, values of the measured SOPs always present an associated error as a consequence of the non ideal set-ups (i.e. rotation stage mis-positioning, retardance values deviation, intensity measurements errors, among others).

Afterwards, if taking into account the effect of noise on to the intensity vector $\boldsymbol{I}$, Eq. (3) and (4) become as it follows:

$$\boldsymbol{S} + \boldsymbol{\Delta S} = \text{A}^{-1}\left(\boldsymbol{I} + \boldsymbol{\Delta I}\right) \tag{5}$$

$$\boldsymbol{S} + \boldsymbol{\Delta S} = \widetilde{\text{A}}^{-1}\left(\boldsymbol{I} + \boldsymbol{\Delta I}\right) \tag{6}$$

where $\boldsymbol{\Delta I}$ is the error associated to the intensity measurements and $\boldsymbol{\Delta S}$ the solution transmitted error.

Noise minimization transmitted through the matrix inversion from the vector $\boldsymbol{I}$ to the solution $\boldsymbol{S}$ is a crucial issue when performing polarimeter optimizations. Consequently, an optimizing criteria needs to be applied. In this work, two well-known indicators are revised and compared: the Condition Number (*CN*) [8] and the Equally Weighted Variance (*EWV*) [9]. Whereas the *CN* quantifies if the matrix A^{-1} is well-conditioned (i.e. how far is from singular matrices), the *EWV* relates to the propagation of errors from the vector $\boldsymbol{I}$ to the solution $\boldsymbol{S}$.

By minimizing the *CN* of a set of possible *A* matrices, the best conditioned matrix (i.e. the closest to an unitary matrix which does not amplify error) is obtained. If *A* is a non-square matrix, the singular value decomposition theorem [13] can be applied. Consequently, the matrix *A* is decomposed as a product of two unitary matrices and a diagonal one. In such a case, the definition of the *CN* is not unique. In this work we have used the definition described by the following relation:

$$\text{CN(A)} = \frac{\sigma_{\max}}{\sigma_{\min}} \tag{7}$$

where $\sigma_{\max}$ and $\sigma_{\min}$ are the maximum and minimum singular values different from zero of the matrix *A*.

As we will prove in section 3, Condition Number is a very useful indicator to measure the condition of a matrix. However, it does not take into account data redundancy. In order to consider the improvement in the measurements provided by data redundancy, we can use the *EWV* indicator, which relates the transmission of the variance from $\boldsymbol{I}$ to $\boldsymbol{S}$:

$$\text{EWV(A)} = \sum_{\text{j=0}}^{\text{R-1}} \frac{1}{\sigma_{\text{j}}^2} \tag{8}$$

where R is the rank of the matrix A and all their singular values σ_j are contributing in the summation of Eq.(8).

The *EWV* indicator provides a helpful estimation of the global error amplification in the solution vector $\boldsymbol{S}$ when some amount of noise is present in the radiometric vector $\boldsymbol{I}$. In addition, this global error is the summation of the specific errors transmitted to each component of the Stokes vector.

3 Polarimeters optimization methodology

In this section, we describe a method useful when performing polarimeter optimizations. This method is based on the indicators shown in section 2 and it is applied for the optimization of a complete non-mechanical polarimeter which is based on two variable LC waveplates. The optical components of such a device are a linear polarizer (PL) at 0º to the laboratory vertical and two LC waveplates oriented at 45º (WP_1) and at 0º (WP_2). The retardance values (φ_1 and φ_2, respectively) of the two LC waveplates are electronically controlled.

This polarimetric system can be used either as a Polarization State Generator (PSG) if it is illuminated with a monochromatic light source or as a Polarization State Detector (PSD) if a monochromatic light beam impinges on it and the intensity is detected by a radiometer. This last configuration is sketched in Fig. 1. It is clear that, given a pair of retardances values (φ_1, φ_2) for the waveplates, a specific SOP is generated by the PSG. Consequently, if a beam with the same SOP is used to illuminate the system when it is acting as PSD, the intensity detected is maximal and any other possible SOP projected over this polarization analyzer gives a lower intensity value.

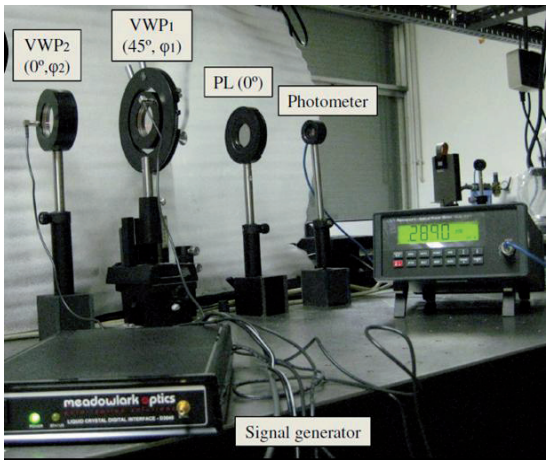

Fig. 1. Set-up of the LC based.

At this point, it is interesting to know which SOPs give maximum flux when projected over the different polarization configurations available with our system. Such SOPs are the same that can be generated by using the polarimeter as PSG. Moreover, those SOPs can be calculated by taking into account Eq. (1) and by multiplying the SOP exiting of a linear polarizer at 0º with the Mueller matrices of the corresponding WP_1 and WP_2 waveplates [12]:

$$\mathbf{S}_{polarimeter} = (S_0, S_1, S_2, S_3)^T = \\ = (1, \cos\varphi_1, \sin\varphi_2 \sin\varphi_1, \cos\varphi_2 \sin\varphi_1)^T \quad (9)$$

The Stokes vector given in Eq. (9) is normalized and consequently, its first parameter S_0 is equal to the unity. Note that the parameters S_1, S_2 and S_3 of the Stokes vector are equivalent to spherical coordinates. It is useful to represent the SOPs given in Eq. (9) upon the Poincaré sphere [12]. In the Poincaré sphere representation, whereas lineal SOPs are mapped on the sphere equator, circular SOPs are represented in the sphere poles. Therefore, any other place upon the Poincaré sphere is mapping a specific elliptical SOP. If we observe Eq. (9), we can easily notice that every locus over the Poincaré sphere can be obtained by properly determining a pair of retardances (φ_1, φ_2). Therefore, any fully polarized polarization analyzer can be used with the set-up shown in Fig. 1, resulting in a system suitable to perform an analysis of Stokes polarimeters optimization (for instance, by minimizing the *CN* indicator).

The *CN* minimization of square matrices A (whose rows are the different polarization analyzers) is conducted by applying a data computing process. It starts with n polarization analyzers randomly chosen. After this, a MATLAB optimization function minimizes the *CN* for different sets of n polarization analyzers, starting from the first random set. Afterwards, the process is repeated N times and in each step, a new set of starting random polarization analyzers is used. The global *CN* with the minimum value and its corresponding A matrix are the solution of the optimization process.

In the particular case of n=4, the solution of the data computing process are four polarization analyzers corresponding to the vertexes of a regular tetrahedron when represented upon the Poincaré sphere. We want to empathize that any of the infinite regular tetrahedrons inscribed into the Poincaré sphere gives the same *CN* value, and so, they are solution for n=4. An example of an obtained regular tetrahedron is plotted at Fig. 2(a), where the surface of the Poincaré sphere has been erased for a better visualization.

The optimization process can also be applied to rectangular matrices A corresponding to n>4 polarization analyzers. We have applied the optimization process for five different numbers n. In particular, the n chosen are the number of the vertexes of the so-called Platonic Solids: n = 4, 6, 8, 12 and 20. After the optimization process, we have obtained sets of polarization analyzers that when represented upon the surface of Poincare Sphere are located at the vertexes of an octahedron (n=6), of a cube (n=8), of an icosahedron (n=12) and of a dodecahedron (n=20), as it can be observed in Fig. 2(b)-2(e). Consequently, the number n of polarization analyzers chosen for the polarimeter optimization relates to the vertexes of regular polyhedrons, if it exists for the specific number n. This result is logical if considering the equidistantly distribution of vertexes in regular polyhedrons (equal edge lengths). In this way, matrices A associated to regular polyhedrons are closer to unitary matrices (which do no amplify error and minimize the

CN number) than matrices *A* containing some of their polarization analyzers closer than others.

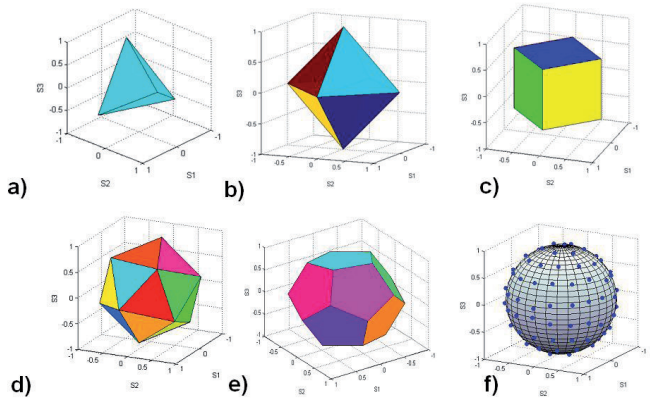

Fig. 2. *CN* minimization for: (a) four, (b) six, (c) eight, (d) twelve, (e) twenty and (f) one hundred polarization analyzers. The vertexes of the regular polyhedrons are located upon the surface of the Poincaré sphere.

At this point, we have applied the optimization process to a number *n* of polarization analyzers with no equivalence into the Platonic Solids group (*n*=100). As expected, the obtained analyzers tend to an equidistant distribution upon the surface of the Poincaré sphere (Fig. 2(f)).

Afterwards, we have analyzed the sensitivity of the *CN* to data redundancy, by studying how this parameter varies as a function of the number of polarization analyzers *n* used. In Fig. 3(a), the optimized *CN* evolution as a function of the number *n* is plotted. In particular, we have calculated the *CN* for nine different optimized polarimeter configurations obtained when using *n*=4, *n*=6, *n*=8, *n*=12, *n*=20, *n*=40, *n*=60, *n*=80 and *n*=100 analyzers. We can easily notice that *CN* is not affected by the increase of the number of analyzers, showing an almost constant value. This is because the redundancy data equally affects the maximum σ_{max} and minimum σ_{min} singular values of the matrix *A* and so, this information is lost in the division of Eq. (7).

Nevertheless, data redundancy in experiments leads to better results and so, an estimation of this improvement becomes crucial. This can be achieved by means of the *EWV* indicator. Subsequently, we have analyzed the behaviour of the *EWV* indicator when increasing the number of polarization analyzers. In particular, for every set of *n* polarization analyzers corresponding to a *CN* minimization obtained by using the MATLAB optimization function, the *EWV* indicator is also calculated (according to Eq. (8)). The results are plotted in Fig. 3(b). We can notice that, the larger the *A* matrix dimensions, the smaller *EWV* values become, by following an asymptotic profile.

Until here, we have conducted simulations leading to optimized Stokes polarimeter configurations (from now on noted as SPC). However, when performing experimental implementations of the obtained SPC, the real polarimeter is not exactly the theoretical one, due to the effect of experimental errors such as vibrations, positioning errors, small manufacturing defaults of the set-up elements, noise added in the radiometric measurements, and so on.

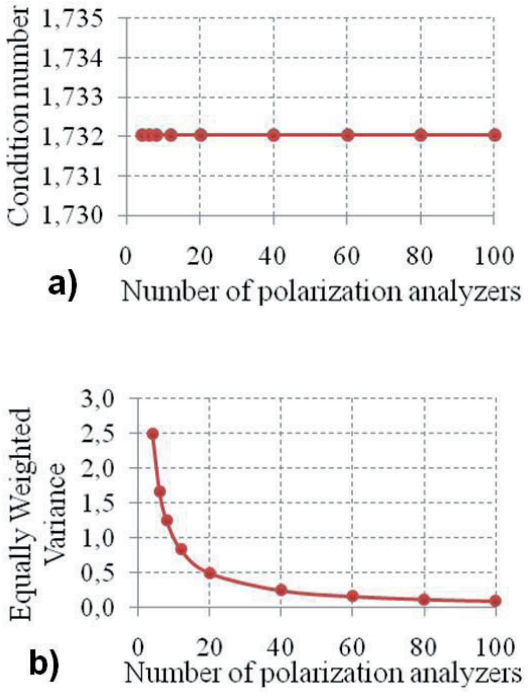

Fig. 3. Analysis of: (a) *CN*; (b) *EWV* as a function of the polarization analyzers number.

At this point, it is interesting to analyze the effect of experimental deviations from a given theoretical optimized SPC on the condition of the system. In fact, we have simulated deviations of the polarization analyzers related to the SPC configuration shown in Fig. 2(a) (regular tetrahedron) and we have calculated the associated variance of the Stokes components, defined in Ref. [14]. One hundred realizations are performed; obtaining one hundred different polarimeter configurations deviated from the theoretical regular tetrahedron. The variations are implemented by generating zero mean uniformly distributed random values with three different amplitudes equal to: 0.1, 0.3, and 0.5.

Figure 4 (a)-(c) shows the variances of the Stokes components corresponding to each different deviated polarimeter. It can be observed that, the larger the amplitude of the simulated deviations, the larger the fluctuations of the variance of the Stokes components. Nevertheless, even for the highest amplitude used (Fig. 4(c)), variance values are small enough to ensure an optimum performance from the associated polarimeter. Consequently, small variations of the polarization analyzers from the ideal polarimeter give an experimental polarimeter leading to values of the *CN* and the *EWV* that do not differ significantly from those associated to the ideal polarimeter and so, leading to still well-conditioned ones.

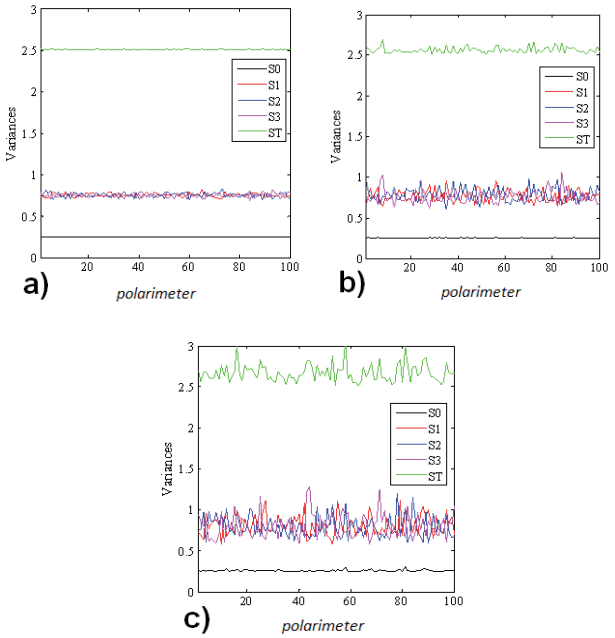

Fig. 4. Numerical simulations of the variances of S_0, S_1, S_2, S_3 and ST for 100 different polarimeters obtained from the optimized theoretical one represented in Fig. 2(a). The deviations are obtained by adding to the polarization analyzers a zero mean, uniformly distributed random numbers with amplitudes (a) 0.1; (b) 0.3; (c) 0.5.

4 Calibration and Implementation of a Stokes polarimeter

In this section, an experimental procedure suitable for the implementation of polarimeters based on variable retarders is described. In particular, different polarimeters configurations are implemented and tested by measuring different incident SOPs. The results obtained are compared with those provided by a commercial polarimeter.

The implemented SPCs are based on the set-up sketched in Fig. 1. Two monopixel Parallel Aligned (PA) LCDs distributed by Meadowlarks, whose retardances depend on the addressed voltage, are used as variable retarders.

The polarimeter configurations chosen are those optimized for n=4, n=20 and n=100 analyzers (Fig. 2(a), (e) and (f) respectively). To experimentally achieve these configurations, it is required to address to each PA LCD the voltage leading to the pair of phases retardances (φ_1, φ_2) which describe the polarization analyzers theoretically obtained. Therefore, a look-up table (LUT) relating the retardance of the LC waveplates with the addressed voltage is required. The waveplate calibration is done by using the set-up shown in Fig. 5.

In particular, a calibrating procedure is performed for each waveplate used. The PA LCD under analysis is set at 45º of the laboratory vertical. In addition, it is sandwiched in between a linear polarizer LP1 (at 0º) and a commercial polarimeter (Analyzer System, PAN 5710VIS, S/N: M60217605) distributed by Thorlabs.

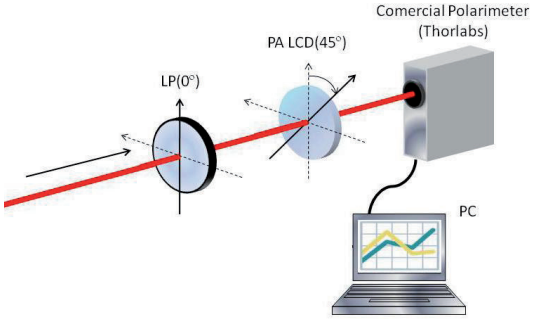

Fig. 5. Experimental set-up for the calibration of the retardance-voltatge look-up table.

Finally, the SOP of the light exiting from the PA LCD is measured by the commercial polarimeter. Moreover, in the M-S formalism, the SOP of the light beam exiting from the LP1+ (PA) LCD optical system is described by the following Stokes vector:

$$\mathbf{S}_{LP1+LCD} = \begin{pmatrix} 1 \\ \cos^2 2\theta + \cos\varphi \sin^2 2\theta \\ (1-\cos\varphi)\sin 2\theta \cos 2\theta \\ \sin\varphi \sin 2\theta \end{pmatrix} \tag{10}$$

where θ is the orientation of the LCD and φ its retardance.

Afterwards, Eq. (10) can be compared to the measurements performed with the commercial polarimeter. In particular, if the exiting SOPs, corresponding to different sampled voltages are known, by fixing a rotation angle θ (45º in this case), an expression for the retardance φ can be deduced from Eq. (10):

$$\varphi = \arctan\left(\frac{S_3 \sin 2\theta}{S_1 - \cos^2 2\theta}\right) \tag{11}$$

where S_1 and S_3 are the Stokes parameters of the SOPs exiting from the LP1+ (PA) LCD system and θ is the orientation of the LCD equivalent retarder fast axis.

In this work, we have measured a set of 20 exiting SOPs for 20 different voltages uniformly distributed from 0.5V to 6V that sweep the entire range of retardations where the LCDs are birefringent active.

Once the phase-voltage values are obtained by means of Eq. (11), a sixth-degree polynomial is applied to interpolate the samples and the calibrated look-up table (LUT) is achieved for every LC waveplate. By means of the calibrated LUTs, the voltages required to implement the optimized polarimeters shown in Fig. 2(a), (e) and (f) are determined.

The polarization analyzers optimization and the waveplates phase calibration provide with potentially well-conditioned polarimeters but as previously stated, experimental inaccuracies become in actual polarimeters slightly different from the desired theoretical ones. In section 3, we have demonstrated that these small deviations from the theoretical values still result in a well-conditioned system, but an experimental calibration of the matrix to be used for an accurate detection is

recommended. To this end, we have employed a method based on the one proposed in [14] and described in [7].

Finally, three implemented complete polarimeter configurations are experimentally tested: the tetrahedron configuration (Fig. 2(a)), the dodecahedron configuration (Fig. 2(e)) and the optimized polarimeter for one hundred polarization analyzers (Fig. 2(f)). The experimental polarimeters have been used for measuring three different incident SOPs: a linear polarized (LP) light beam at 70º of the lab vertical, a right-handed circular polarized light (CP) and an elliptical polarized light beam (EP). The measurements are compared to the provided by the commercial polarimeter distributed by Thorlabs. The results obtained (in terms of azimuth α and ellipticity ε) are given in Table 1, being in each case, the average of 100 measurements of the same incident SOP. Thus, the standard deviation σ corresponding to a population of 100 samples is also calculated. Note that azimuth values α of circular polarized light are not evaluated because there is not a privileged orientation of the polarization ellipse in such a polarized light.

A good agreement between results given by the implemented polarimeter configurations and those given by the commercial polarimeter can be easily noticed. This agreement between data is observed for the detection of three different SOPs notably separated upon the Poincare sphere, showing the suitability of the optimization performed.

Note that the standard deviation values associated to the measurements performed by using the commercial polarimeter are smaller than the ones obtained by using the three optimized polarimeter configurations of Table 1. This is because of the large redundancy data generated by the mechanical commercial polarimeter. Nevertheless, from the results given in Table 1, we can easily notice that a LC-based polarimeter can also increase its repeatability (decrease the standard deviation value of its measurements) by adding polarization analyzers.

As an example, the standard deviations obtained by using the n=100 optimized polarimeter are of the same order than the ones given by the commercial polarimeter. Finally, we want to emphasize that the experimental results given in Table 1 are an important indicator of the validity of the optimization methodology provided in this work.

Table 1. Azimuth α and Ellipticity ε values corresponding to three different measured SOPs

	Optimized Tetrahedron		Optimized Dodecahedron	
	$\alpha\pm\sigma(\alpha)$	$\varepsilon\pm\sigma(\varepsilon)$	$\alpha\pm\sigma(\alpha)$	$\varepsilon\pm\sigma(\varepsilon)$
LP	70.34±0.29	0.31±0.28	69.56±0.13	0.06±0.14
CP	-	44.63±0.18	-	44.31±0.11
EP	44.95±0.42	24.24±0.29	45.59±0.16	23.49±0.11
	n=100 Optimized Polarimeter		Commercial Polarimeter	
	$\alpha\pm\sigma(\alpha)$	$\varepsilon\pm\sigma(\varepsilon)$	$\alpha\pm\sigma(\alpha)$	$\varepsilon\pm\sigma(\varepsilon)$
LP	70.08±0.05	0.18±0.06	69.99±0.02	0.05±0.02
CP	-	44.89±0.05	-	44.72±0.02
EP	45.94±0.10	23.63±0.09	44.43±0.04	23.58±0.02

5 Conclusions

This work provides an optimization and implementation of different Stokes polarimeter configurations based on two monopixel Parallel Aligned Liquid Crystal Displays.

We have achieved some optimal polarimeter configurations by minimizing the Condition Number indicator. The n polarization analyzers obtained for a specific polarimeter optimization, are located (when plotted upon the Poincare sphere surface) at the vertexes of the Solid Platonic with a number of vertexes equal to n (if exists).

We have also studied the usefulness of the Equally Weighted Variance and of the Condition Number indicators for evaluate the improvement in measurements provided by data redundancy. Whereas the *CN* indicator is not affected by data redundancy, the *EWV* shows an asymptotic behaviour as a function of this parameter. In particular, the larger the data redundancy, the smaller the *EWV* indicator value.

In addition, we have verified that small deviations from the optimal configuration lead to still well conditioned polarimeters. We have carried out an experimental calibration of the polarimeter configuration. Finally, we have implemented and tested the optimal polarimeters, where an excellent agreement with the results obtained by using the commercial polarimeter is observed.

References

1. M. Anastasiadou, A. De Martino, D. Clement, F. Liège, B. Laude-Boulesteix, N. Quang, J. Dreyfuss, B. Huynh, A. Nazac, L. Schwartz and H. A. S. Cohen, Phys. Stat. Sol., **5** (2008)
2. J.L. November and L.M. Wilkins, Proc. SPIE, **2265** (1992).
3. S. Firdous and M. Ikram, Proc. of the SPIE-OSA Biomedical , **6632** (2007)
4. R. A. Chipman, *Polarimetry*, in Handbook of Optics, New York (1995)
5. E. Garcia-Caurel, A. De Martino and B. Drévillon, Thin Solids Films, **455** (2004)
6. J. M. Bueno, J. Opt. A: Pure Appl. Opt., **2** (2000).
7. A. Peinado, A. Lizana, J. Vidal, C. Iemmi and J. Campos, Opt. Express (to be published)
8. P. Taylor, *Theory and Applications of Numerical Analysis*, London, (1974)
9. D.S. Sabatke, M.R. Descour, E.L. Dereniak, W.C. Sweatt, S.A. Kemme and G.S. Phipps, Opt. Letters, **25** (2000)
10. R. C. Jones, J. Opt. Soc. Am. A **31**(1941).
11. R.M.A. Azzamm N.M. Bashara, *Ellipsometry and Polarized light*, Amsterdam, (1977)
12. D. Goldstein, *Polarized Light*, Marcel Dekker, NY, (2003).
13. G. E. Forsythe, M.A. Malcolm and C.B. Moler, *Computer Methods for mathematical computations*, Jersey, (1977)
14. J. Zallat, S. Aïnourz and M.Stoll, J.Opt.A: Pure Appl. Opt., **8** (2006)

15. S.R. Davis, R. Uberna and R. A. Herke, United State Patent, patent US **6744509 B** (2004)

Acknowledgments

We acknowledge financial support from Spanish Ministerio de Educación y Ciencia (FIS2009-13955-C02-01) and Generalitat de Catalunya (2006PIV00011). C. Iemmi acknowledges support from Univ. Buenos Aires and CONICET (Argentina).